Journal of Physical Science and Application 5 (6) (2015) 377-395
doi: 10.17265/2159-5348/2015.06.001

Solution of Self-similar Equations of the k-ε Model in the Shear Turbulent Mixing Problem and Its Numerical Simulation

Vyacheslav P. Statsenko, Yulia V. Tret'yachenko and Yury V. Yanilkin*
Russian Federal Nuclear Centre, VNIIEF, Sarov, 607200, Russia

Abstract: The paper presents the k-ε model equations of turbulence with a single set of constants chosen by the authors, which is appropriate to simulate a wide range of turbulent flows. The model validation has been performed for a number of flows and its main results are given in the paper. The turbulent mixing of flow with shear in the tangential velocity component is discussed in details. An analytical solution to the system of ordinary differential equations of the k-ε model of turbulent mixing has been found for the self-similar regime of flow. The model coefficients were chosen using simulation results for some simplest turbulent flows. The solution can be used for the verification of codes. The numerical simulation of the problem has been performed by the 2D code EGAK using this model. A good agreement of the numerical simulation results with the self-similar solution, 3D DNS results and known experimental data has been achieved. This allows stating that the k-ε model constants chosen by the authors are acceptable for the considered flow.

Key words: The k-ε model of turbulent mixing, shear turbulent mixing, self-similar equations, numerical simulation.

Nomenclature

If not additionally specified, the following notations are used in this paper:

t	Time
L	Length
u	Mass velocities
ρ	Density
e	Specific energy
T	Temperature
R	Reynolds stress tensor
s	Specific entropy
α	Mass fraction
P	Pressure
P_T	Turbulent pressure
k	Turbulent energy
ε	Turbulent energy dissipation rate
D	Kinematic coefficient of Turbulent viscosity
G_1	Shear generation of turbulence
G_2	Gravitation generation of Turbulence
$A \equiv (\rho_2 - \rho_1)/(\rho_2 + \rho_1)$	Atwood number
$c_\mu, \sigma_m, \sigma_h, \sigma_k, \sigma_\varepsilon, c_{\varepsilon 1}, c_{\varepsilon 2}, c_{\varepsilon 3}$	k-ε model coefficients

*Corresponding author: Yury Vasilyevich Yanilkin, professor, research field: computational mathematics.

1. Introduction

The k-ε model is one of the most successful models of turbulence and it is commonly used in engineering practice and research activities. Similarly to any other phenomenological model of turbulence, the k-ε model has a set of semi-empirical coefficients. Usually, they can be found by solving the simplest self-similar problems, for which experimental data is available. In the self-similar stage, the effect of initial conditions, or some other factors introducing additional parameters to the description of flow is eliminated. The choice of model constants is made, as a rule, for a certain type of flows caused by the Rayleigh-Taylor, Kelvin-Helmholtz, or Richtmyer-Meshkov instabilities and they are different for various flows. However, in practice, it's not possible to vary model constants for different types of flows and there is a need in a single set of constants suitable for a wide range flows. So, a representative class of flows is required to select constants. Of course, the chosen constants, though it is universal to a sufficient extent,

may be of a higher, or a lower accuracy (depending on each particular flow) in comparison with a specialized set of constants for a given flow. For the code in use and for the chosen set of constants, it is better to have a comprehensive range of test problems.

Paper [1] considers several simplest flows, for which both experimental data and 3D ILES results are available, and certain semi-empirical coefficients for the k-ε model implemented in the EGAK code [2] have been selected by comparing with this data. Some of these flows are considered in the present paper, the numerical simulation results have been also obtained using the standard set of constants.

One of such problems is the classic problem of shear mixing in a plane mixing layer. The problem was studied analytically, experimentally, numerically in many papers [3-11]. For the self-similar regime, this flow type was numerically studied by the authors with the 2D ILES [3] and 3D ILES [4] methods. However, the 3D ILES [5], 3D LES [12], and 3D DNS [13, 14] simulations on finer grids than those used in Ref. [4] demonstrated a significant spread in results and the necessity of studying this type of flows in details.

The principal objective of the paper is to justify the previously selected set of constants of the k-ε model for the flow type of interest. The authors had found an exact solution to the k-ε model's self-similar equations using these constants and then the solution was used for the EGAK code verification (it may be also used for the verification of any other code). The second objective is to validate the k-ε model by comparing the solution found with the available experimental data and 3D ILES results. Additionally, correctness of the chosen model constants was confirmed by comparing with results of simulations using the standard set of model coefficients.

For ease of understanding by the readers, we also give an approximate solution to the problem from paper [1], for comparison. We performed a more correct post-processing of the available 3D ILES results and studied a broader range of experimental data [6-11].

2. The Proposed k-ε Model and Some Test Problems

2.1 Principal Equations of the k-ε Model

Consider weakly compressible flows with a negligible molecular viscosity (large Reynolds numbers). The CFD equations in the presence of turbulent mixing can be written as:

$$\partial\rho / \partial t + div\left(\rho\vec{u}\right) = 0 \tag{1}$$

$$\frac{\partial}{\partial t}(\rho u_i) + \frac{\partial}{\partial x_k}\left(\rho u_i u_k\right) = -\frac{\partial P}{\partial x_i} + \frac{\partial \sigma_{ikT}}{\partial x_k} + g_i\rho \tag{2}$$

where, $\vec{g}$ is the mass force (gravity) acceleration.

The Reynolds stress tensor, $\sigma_{ijT} \equiv -\overline{\rho}\cdot\overline{u_i'u_j'}$ is approximated, as usually:

$$\sigma_{ijT} = \rho D\left(\frac{\partial u_j}{\partial x_i} + \frac{\partial u_i}{\partial x_j} - \frac{2}{3}\delta_{ji}\frac{\partial u_k}{\partial x_k}\right) - P_T\delta_{ji} \tag{3}$$

Here, $P_T = 2/3\rho k$ is turbulent pressure, k is turbulent energy. The kinematic coefficient of turbulent viscosity is:

$$D = c_\mu k^2 / \varepsilon \tag{4}$$

where, ε is the turbulent energy dissipation rate.

The equation of specific energy, e = e(ρ, P) looks like

$$\frac{\partial}{\partial t}(\rho e) + \frac{\partial}{\partial x_n}\left(\rho u_n e - P a_n + Q_n^T\right) = \rho\varepsilon - P\frac{\partial u_n}{\partial x_n} - G_2 \tag{5}$$

where, the molecular flow of heat is assumed to be negligibly small:

$$G_2 = a_k\frac{\partial P}{\partial x_k},\quad a_i \equiv \frac{\overline{\rho' u_i'}}{\rho} = -\frac{D}{\rho\sigma_h}\left(\frac{\partial\rho}{\partial s}\right)_P\frac{\partial S}{\partial x_k}$$

$$Q_n^T = -\frac{\rho D}{\sigma_h}\left(\frac{\partial e}{\partial s}\right)_P\frac{\partial S}{\partial x_k},$$

S is specific entropy. For an ideal gas with a constant value of γ, we can write:

$$a_k = \frac{D}{\sigma_h}\left(\frac{1}{\gamma p}\frac{\partial P}{\partial x_k} - \frac{1}{\rho}\frac{\partial\rho}{x_k}\right). \tag{6}$$

The mass fraction equation for one of the two components looks like:

$$\frac{\partial}{\partial t}(\alpha\rho)+\frac{\partial}{\partial x_k}\left(\alpha\rho u_k\right)= \frac{\partial}{\partial x_k}\left(\frac{\rho D}{\sigma_m}\left(\frac{\partial\alpha}{\partial s}\right)_{|p}\frac{\partial s}{\partial x_k}\right) \quad (7)$$

Here, the molecular diffusion flow is also negligible.

The EOS (Equation of state) for a mixture of ideal gases has the form:

$$P = RT\rho/\mu;\quad \mu\equiv\alpha/\mu_1+(1-\alpha)/\mu_2 \quad (8)$$

Differential equations for the turbulent energy and dissipation rate look like:

$$\frac{\partial}{\partial t}(\rho k)+\frac{\partial}{\partial x_k}(\rho k u_k)= (G_1+G_2)-\rho\varepsilon+\frac{\partial}{\partial x_k}\left(\frac{\rho D}{\sigma_k}\cdot\frac{\partial k}{\partial x_k}\right) \quad (9)$$

$$\frac{\partial}{\partial t}(\rho\varepsilon)+\frac{\partial}{\partial x_k}(\rho\varepsilon u_k)= \frac{\varepsilon}{k}\left(c_{\varepsilon1}G_1+c_{\varepsilon3}G_2-c_{\varepsilon2}\rho\varepsilon\right)+\frac{\partial}{\partial x_k}\left(\frac{\rho D}{\sigma_\varepsilon}\frac{\partial\varepsilon}{\partial x_k}\right) \quad (10)$$

where, G_1 is the shear generation of turbulence:

$$G_1=\sigma_{jkT}\cdot\partial u_j/\partial x_k. \quad (11)$$

Eqs. (1)-(11) contain phenomenological coefficients: $c_\mu, \sigma_m, \sigma_h, \sigma_k, \sigma_\varepsilon, c_{\varepsilon1}, c_{\varepsilon2}, c_{\varepsilon3}$. Various authors use different values of these coefficients for particular flows (see, for example, [15-18]). However, note that there is a "standard" set of constants used in a number of papers [16-19]: $c_\mu = 0.09$, $\sigma_m = \sigma_h = 0.9$, $\sigma_k = 1$, $\sigma_\varepsilon = 1.3$, $c_{\varepsilon1} = c_{\varepsilon3} = 1.44$, $c_{\varepsilon2} = 1.92$.

The values of constants selected for the EGAK code for the full set of the simplest flows discussed below with regard to the modern 3D simulations are, as follows: c_μ =0.12, $\sigma_k = \sigma_\varepsilon$ =3/4, $c_{\varepsilon1}$ =1.15, $c_{\varepsilon3}$ =1, $\sigma_h = \sigma_m = 1/1.7$, $c_{\varepsilon2}$ = 1.7. They differ from the standard ones.

2.2 Decay of Homogeneous Isotropic Turbulence

It follows from Eqs. (10) and (11) for the given problem that

$$\partial k/\partial t = -\varepsilon;\qquad \partial\varepsilon/\partial t = -c_{\varepsilon2}\varepsilon^2/k \quad (12)$$

hence,

$$\varepsilon/\varepsilon_0 = \left(k/k_0\right)^{c_{\varepsilon2}} \quad (13)$$

From Eqs. (12) and (13) we obtain:

$$k/k_0 = \left(t/t_0\right)^{-m};\quad t_0\equiv mk_0/\varepsilon_0. \quad (14)$$

Here, $m = 1/\left(c_{\varepsilon2}-1\right)$.

For the spatial scale of turbulence, $\Lambda = k^{3/2}/\varepsilon$ with regard to Eq. (14) we have:

$$\Lambda/\Lambda_0 = \left(t/t_0\right)^{\delta};$$
$$\delta = 1-m/2;\quad \Lambda_0\equiv k_0^{3/2}/\varepsilon_0 \quad (15)$$

The decay law for homogeneous isotropic turbulence – m = 10/7, δ = 2/7 – following from the theoretic considerations in [20] is confirmed by results of experiments [21]. For the values of $c_{\varepsilon2}$ used in the given paper the corresponding values of m and δ are given in Table 1.

As we can see, these values for $c_{\varepsilon2}$ =1.7 agree with the data from [20], [21], while the values for $c_{\varepsilon2}$ =1.92 in the standard model [16-18] significantly differ.

2.3 Neutrally Stratified Turbulent Boundary Layer

This problem has a single velocity component, $u_x = u_x(y)$, where, y is the distance to a rigid wall. Then, $G_2 = 0$, $\Lambda \sim k^{3/2}/\varepsilon \sim y$ and a typical time scale is $\tau \sim \Lambda/u_* \sim y$, where the dynamic velocity is $u_*^2 \equiv D\partial u_x/\partial y = const$ and we take $\partial u_x/\partial y > 0$, $\rho = 1$ for definiteness. This means τ is small near the wall, i.e. the turbulent flow becomes steady-state. Eq. (2) gives $\partial\sigma_{xy}/\partial y = 0$ for this case, or, with regard to Eq. (4),

$$\sigma_{xy} = -D\partial u_x/\partial y \equiv -u_*^2 = const,$$

this agrees with our previous assumption. $\partial u_x/\partial y \sim u_*/y$ in this case and, hence, $D \sim y$.

Table 1 Parameters m and δ of the decaying homogeneous isotropic turbulence for different values of coefficient cε2.

$c_{\varepsilon2}$	m	δ
1.92	1.087	0.4565
1.7	10/7	2/7

However, $D \sim \Lambda\sqrt{k}$ and, hence, $k = const$ near the wall. Then, it follows from Eqs. (10) and (12) that

$$G_1 = D\left(\partial u_x / \partial y\right)^2 = \varepsilon . \qquad (16)$$

Eq. (11) can be written as

$$\frac{\varepsilon^2}{k}\left(c_{\varepsilon 1} - c_{\varepsilon 2}\right) + \frac{\partial}{\partial y}\left(\frac{D}{\sigma_\varepsilon}\frac{\partial \varepsilon}{\partial y}\right) = 0 \qquad (17)$$

With regard to Eqs. (6) and (16), we have $\varepsilon / k = \sqrt{c_\mu} \cdot \partial u_x / \partial y$.

Thus, Eq. (17) can be written as

$$C_f f^2 = \frac{\partial^2 \ln f}{\partial y^2} \qquad (18)$$

where,

$$f \equiv \partial u_x / \partial y; \quad C_f \equiv \left(\kappa_K / u_*\right)^2; .$$
$$\kappa_K \equiv c_\mu^{1/4}\sqrt{\left(c_{\varepsilon 2} - c_{\varepsilon 1}\right)\cdot \sigma_\varepsilon}$$

The solution to Eq. (18) has the form

$$u = u_* / \kappa_K \ln\left(y / h_0\right), \qquad (19)$$

where, h_0 is either a height of irregularity, or a laminar sub-layer width. We see from Eq. (19) that κ_K is Karman constant. Its values for different sets of empirical coefficients used in this paper are given in Table 2.

According to the experimental data from Ref. [22], κ_K = 0.4 ± 0.04. It is clear from Table 2 that both option 1 and option 2 satisfactorily agrees with this data.

2.4 Gravitational Mixing of a Plane Interfacial Layer

Consider two half-spaces separated at initial time by plane z = z_c = 0 and filled out with incompressible fluids (gases) at rest with densities ρ_1=1 and ρ_2=n=3. The gravitational acceleration, g_z = − 1 ≡ − g is directed from a heavy material to a light material. The self-similar problem of gravitational turbulent mixing in the layer described above is considered. We think that "gravitational turbulent mixing" is a more appropriate term than "mixing by Rayleigh-Taylor instability", because in the nonlinear stage of the Rayleigh-Taylor instability development the shear instability is of an equal importance for the direct 3D numerical simulation.

The interface $z = z_0$ is at rest in the coordinate system in use. Introduce quantity $L_t \equiv z_2 - z_1$, which is the TMZ width in direction z determined by points z_1, z_2 at which a small enough value ($\varepsilon \approx 0.01$) of concentration disturbance is achieved: $\alpha_2(z_1) = \varepsilon$, $\alpha_2(z_2) = 1 - \varepsilon$, α_2 is the mass fraction of material with the initial density ρ_2 = n.

The problem of turbulent mixing under a constant gravity (constant acceleration) on a plane interface of two incompressible fluids (gases) was experimentally investigated and described in a number of papers see [23-27]. It turns out that quantity *n* really does not influence the dimensionless quantity α_b characterizing the penetration of a light fluid (bubbles) into a heavy fluid: $z_2 - z_c = \alpha_b \cdot A \cdot g \cdot t^2$. The authors of [26] obtained α_b = 0.078. In some other experiments, the value of α_b is lower, for example, α_b = 0.06-0.07 in [23, 24]. In the experiments described in [27] and in the later experiments [28, 29] the α_b values are far less.

The problem was numerically studied in a number of works [25, 30-35] by performing 2D and 3D simulations with the DNS method. Simulations using a sufficiently fine grid give noticeably lower TMZ growth rates than those in experiments [23-27]. As it is shown in [33], such discrepancy is owing to the fact that measurement results were processed with a large weight of the initial non-self-similar time interval.

Table 2 The values of κ_K for two sets of empirical coefficients.

Option No.	c_μ	$c_{\varepsilon 1}$	σ_ε	$c_{\varepsilon 2}$	κ_K
1	0.09	1.44	1.3	1.92	0.433
2	0.12	1.15	3/4	1.7	0.378

Results of simulations with the EGAK code using the k-ε model and various experimental and calculated data are given in Table 3. Note, first, that we performed data post-processing in a more correct fashion (similarly to the simulation result post-processing in [32, 33]) using experimental data from [27] for n=2.83 and obtained α_b =0.031 ÷ 0.033 (instead of $\alpha_b \approx 0.05$ given in this work), which agrees better with 3D simulation results in [33-35]. Also, the EGAK results (option 2) approximately agree with them, while simulations with the standard coefficients (option 1) give us the α_b values, which are lower by an order of magnitude in comparison with experiments and 3D simulation results.

2.5 Gravitational Mixing in a Light (Heavy) Plane Layer

A light (heavy) plane layer of density ρ_1 and initial width d surrounded by a fluid of density ρ_0 is in the gravity field with acceleration g. The self-similar solution is at $L_t / d \to \infty$ (L_t is the layer width at time t), for the light layer we find it in the form (for the heavy layer, variations are clear):

$$\frac{\rho}{\rho_0} = 1 - \frac{d\varphi(\eta)}{L_t(t)}\left(1 - \frac{\rho_1}{\rho_0}\right), \ \eta \equiv \frac{z - z_d}{L_t}. \qquad (20)$$

Quantity b is defined according to Ref. [32]:

$$b \equiv \frac{d\tilde{L}}{dt}; \qquad \tilde{L} \equiv \frac{L_t}{\sqrt{dg(1-\rho_1/\rho_0)}} \equiv \frac{L_t}{B}.$$

Here,

$$B \equiv \sqrt{dg\left(1 - \rho_1 / \rho_0\right)} \qquad (21)$$

The values of quantity b in the self-similar regime in the EGAK code simulations with varying coefficients are given in Table 4. It is clear from data in Table 4 that the b width measurement results [36] are closer to the option 2 results of simulations. At the same time, the option 1 simulations give the values of b which are several times lower than the experimental results in Ref. [36].

3. Analytical Solutions for the Self-Similar Regime of an Incompressible Shear Flow of Uniform Density

3.1 Principal Equations

The flow of interest has only one velocity component, u_x varying in the y coordinate alone. The molecular viscosity is considered to be negligible. The flow density has constant value, ρ = 1 everywhere. For this problem, equations from subsection 1.1 have the following form:

Table 3 The value of α_b in the problem of gravitational mixing of a plane interfacial layer, A ≈ 0.5.

Option No.	c_μ	$c_{\varepsilon 3}$	σ_ε	σ_k	σ_h	$c_{\varepsilon 2}$	α_b
1	0.09	1.44	1.3	1	0.9	1.92	0.0019
2	0.12	1	3/4	3/4	1/1.7	1.7	0.0235
Experiments [26]							0.078
Experiments [27]							0.051 ± 0.005
Experiments [28]							0.04
Experiments [29]							0.03-0.04
3D simulations [33]							0.028
3D simulations [34]							0.022-0.03
3D simulations [35]							0.027

Table 4 The coefficients values and simulation results for the problem of mixing in a light layer.

Option No.	c_μ	$c_{\varepsilon 3}$	σ_h	σ_k	σ_ε	$c_{\varepsilon 2}$	b
1	0.09	1.44	0.9	1	1.3	1.92	0.1
2	0.12	1	1/1.7	3/4	3/4	1.7	0.36
Experiments [36]							0.35 ÷ 0.37

• Discontinuity equation (it is satisfied automatically in the given case)

$$\partial u_k / \partial x_k = 0,$$

• Equations of motion

$$\partial u_x / \partial t = \partial \sigma_{xy} / \partial y \qquad (22)$$

The Reynolds stress tensor, $\sigma_{ij} \equiv -\overline{\rho} \cdot \overline{u_i' u_j'}$ is approximated, as usually:

$$\sigma_{xy} = D \partial u_x / \partial y, \qquad (23)$$

where, $D = c_D k^2 / \varepsilon$ is coefficient of turbulent viscosity, k is turbulent energy, ε is the turbulent energy dissipation rate

The turbulent energy equation looks like

$$\frac{\partial k}{\partial t} = G_1 - \varepsilon + \frac{\partial}{\partial y}\left(c_k D \frac{\partial k}{\partial y} \right), \qquad (24)$$

equation for the turbulent energy dissipation rate has the form:

$$\frac{\partial \varepsilon}{\partial t} = \frac{\varepsilon}{k}\left(c_{\varepsilon 1} G_1 - c_{\varepsilon 3} \varepsilon \right) + \frac{\partial}{\partial y}\left(c_\varepsilon D \frac{\partial \varepsilon}{\partial y} \right) \qquad (25)$$

Here, the shear generation of turbulence is

$$G_1 = \sigma_{ji} \partial u_j / \partial x_i = D\left(\partial u_x / \partial y \right)^2 \qquad (26)$$

Eqs. (22)-(26) have coefficients c_μ =0.12, $\sigma_k = \sigma_\varepsilon$ =3/4, $c_{\varepsilon 1}$ =1.15, $c_{\varepsilon 2}$ =1.7.

3.2 Equations of the k-ε Model for the Self-Similar Regime of Shear Mixing in a Plane Interfacial Layer

The model considered here can be used to describe a self-similar shear flow, such as the flow occurring in the initial section of a mixing layer at the edge of a jet flowing out of a nozzle, when the ratio between the jet velocity, u_1 and the nozzle velocity relative to the surrounding medium, u_2 is close to 1: $m \equiv u_1 / u_2 \approx 1$. Another example is a homogeneous flow from a spacer plate having velocities u_1 and u_2 relative to the plate (such experiments were used in Refs. [6-11] to study a plane layer of mixing).

In the coordinate system of fluid with a uniform density the problem becomes one-dimensional and unsteady, i.e. in the self-similar regime the plane mixing layer's width grows linearly with time in proportion to the velocity difference u_0 between the jet velocity and the surrounding medium velocity. (For the detailed information, see Appendix A)

Introduce self-similar variables:

$$u_x \equiv dx / dt = u_0 \cdot f(\chi) / 2,$$

$$k = u_0^2 \cdot E(\chi), D = u_0^2 \cdot t \cdot d(\chi), \ \chi \equiv y / (u_0 t). \qquad (27)$$

The boundary condition for the tangential velocity u_x varying in the y coordinate only is

$$u_x = \begin{cases} u_0 / 2, & y \geq y_2 \\ -u_0 / 2, & y \leq y_1 = -y_2 \end{cases} \qquad (28)$$

where, $u_0 = u_2 - u_1$.

Write Eqs. (22) and (23) for the self-similar regime assuming that $v \equiv f'$:

$$\chi v + (dv)' = 0. \qquad (29)$$

Write Eqs. (24) and (25) with regard to (26) for the self-similar regime:

$$\chi E' + d \cdot v^2 / 4 - c_D e + c_k \left(d \cdot E' \right)' = 0 \qquad (30)$$

$$e + \chi \cdot e' + e$$

$$\cdot (c_{\varepsilon 1} \cdot d \cdot v^2 / 4 - c_{\varepsilon 3} \cdot c_D \cdot e) / E + c_\varepsilon \cdot \left(d \cdot e' \right)' = 0. \qquad (31)$$

Here,

$$e \equiv E^2 / d. \qquad (32)$$

3.3 An Approximate Solution

To find an approximate solution, consider Eqs. (24) and (25) in the central part of TMZ (for χ=0), where the first-order derivatives of quantities k, ε, D become zeroes and write Eq. (24) for the self-similar regime in the form:

$$d \cdot v^2 / 4 - c_D E^2 / d + c_k \left(d \cdot E' \right)' = 0 \qquad (33)$$

Accept approximations

$$K = E / d \approx const, \qquad (34)$$

$$v \approx const. \qquad (35)$$

Then, it flows from Eq. (29) that

$$d = \left(\chi_1^2 - \chi^2\right)/2, \quad (36)$$

and from Eq. (32) we obtain $E'' = -K = \left(c_D K^2 - v^2/4\right)/c_k$, i.e.

$$v = 2\sqrt{K\left(c_D K + c_k\right)} \quad (37)$$

Eq. (25) for the self-similar regime, with regard to Eqs. (34)-(37), gives us

$$K = \frac{1 - c_\varepsilon + c_{\varepsilon 1} c_k}{c_D\left(c_{\varepsilon 3} - c_{\varepsilon 1}\right)} \quad (38)$$

Take $\mathrm{f}(\chi_2) = 1; \quad \mathrm{f}(\chi_1) = -1$, and $\mathrm{L} = \mathrm{y}_2 - \mathrm{y}_1$ (TMZ width) and obtain

$$v = \frac{df}{d\chi} \approx \frac{2A_v}{\chi_2 - \chi_1} = \frac{A_v}{|\chi_1|}, \quad (39)$$

$$\hat{\dot{L}} \equiv \frac{1}{u_0} \cdot \frac{dL}{dt} = \chi_2 - \chi_1 = \frac{2A_v}{v} = \frac{A_v}{\sqrt{K\left(c_D K + c_k\right)}}, \quad (40)$$

where, the correction coefficient, $A_v > 1$ takes into account that the value of $v = f / d\chi \approx 2A_v / \left(\chi_2 - \chi_1\right)$ at the TMZ center (which is considered here) exceeds the average value of this quantity in TMZ, $\bar{v} = \overline{df/d\chi} = 2/\left(\chi_2 - \chi_1\right)$.

It follows from Eqs. (34) and (36) that the E maximum is $E_m = K\chi_1^2/2$ and with regard to Eq. (40) it allows finding the reduced turbulent energy maximum.

$$E_m = \frac{KA_v^2}{2v^2} = \frac{A_v^2}{8\left(c_D K + c_k\right)}. \quad (41)$$

A more complicated approximate analytical solution to the $k-\varepsilon$ model equations , when v is a function of χ, is given in Ref. [19].

3.4 Solution of Self-Similar Equations

Write the second-order derivatives using Eqs. (30) and (31):

$$E'' = \frac{c_D e - \chi E' - d \cdot v^2/4 - c_k d' \cdot E'}{c_k d}, \quad (42)$$

$$e'' = \frac{\frac{e}{E}\left(c_{\varepsilon 3} c_D e - \frac{c_{\varepsilon 1}}{4} d \cdot v^2\right) - e - \chi e' - c_\varepsilon d' \cdot e'}{c_\varepsilon d}. \quad (43)$$

Solutions to Eqs. (29), (42) and (43) can be found numerically in the two ways: by integrating these equations in intervals χ =0 to $\chi = \chi_2$ and $\chi = \chi_1$ to χ =0. Consider the first way of integrating.

The boundary condition at point $\chi = 0$ is

$$E' = d' = 0. \quad (44)$$

It also follows from Eqs. (45) and (30) that $v' = e' = 0$.

At the same point, set nonzero values of quantities (the approximate analytical solution is taken for the first approximation):

$$v = v_0 > 0, \quad d = d_0 > 0, \quad E = E_0 > 0. \quad (45)$$

And, according to Eqs. (42) and (43), the second-order derivatives are:

$$E_0'' = \frac{c_D e_0 - d_0 v_0^2/4}{c_k d_0},$$

$$e_0'' = \frac{\frac{e_0}{E_0}\left(c_{\varepsilon 3} c_D e_0 - \frac{c_{\varepsilon 1}}{4} d_0 v_0^2\right) - e_0}{c_\varepsilon d_0}.$$

Integrate Eqs. (29), (42) and (43) between point χ =0 and point $\chi = \chi_2$, where the values of quantities d and E are $d(\chi_2) = E(\chi_2) = 0$. During the integration find d using Eq. (32) and then find v using the solution to Eq. (29)

$$v = \frac{d_0 v_0}{d} \cdot \exp\left\{-\int_0^\chi \frac{\chi}{d} \cdot d\chi\right\}.$$

Vary the values of quantities in (45) to achieve zero values of d and E at the same time. In general, one more boundary condition following from (27), (28) is not satisfied in this case $f(\chi_2) = 1$. However, it is easy to show that for the two solutions with different values $\chi = \chi_2$ and $\tilde{\chi} = \tilde{\chi}_2$ the scale transformation takes place:

$$\chi = \frac{\tilde{\chi}}{\Delta}, \quad v = \tilde{v}, \quad f = \frac{\tilde{f}}{\Delta}, \quad d = \frac{\tilde{d}}{\Delta^2}, \quad E = \frac{\tilde{E}}{\Delta^2}, \quad (46)$$

where, $\Delta = \int_0^{\tilde{\chi}_2} \tilde{v} \cdot d\tilde{\chi} = \tilde{f}(\tilde{\chi}_2)$.

Thus, use solution $\tilde{v}$, $\tilde{d}$, $\tilde{E}$ giving us $\tilde{\chi} = \tilde{\chi}_2$, under which $\tilde{f}(\tilde{\chi}_2) = \Delta \neq 1$, and by making transformation (46) obtain the solution satisfying the

condition $f(\chi_2)=1$. For this purpose, vary the values of v_0 and ratio d_0/E_0, which do not change during the transformation (46).

4. Numerical Simulation Using the k-ε Model

4.1 Problem Setting

A planar interface of two incompressible fluids has a tangential velocity discontinuity, $\Delta u_x \equiv u_0 = 1$ (Fig. 1): above the interface corresponding to coordinate y = 1, the fluid (gas) moves parallel to the interface with the velocity $u_x = u_0/2$ and below the interface its velocity is $u_x = -u_0/2$. The velocity on the interface is $u_x = 0$. Boundary conditions on the left and on the right of the computational domain are periodic, the top and bottom boundaries are "rigid walls". Initially, the both domains are filled with ideal gases with γ = 1.4 and density ρ = 1 under pressure P_0 = 10, i.e. the flow is close to the incompressible one. To check such conditions for sufficiency, simulations with pressure P_0 = 50 were also performed using a grid of N = 400 points (N is the number of points in domain along *y* axis). The initial values of turbulence quantities, k = 0.001 and ε = 0.025, are set at the interface (in one layer of cells on each side of the interface). In all other cells, the initial values of these quantities are $k = \varepsilon = 10^{-11}$.

Simulations were performed using a square Eulerian grid by varying the number of cells along *y* axis (see Table 5).

4.2 Results of the 2D Simulations, Comparison with the Solutions of Self-Similar Equations and Measurements

The resulting profiles of the solutions described in subsection 3.4 are shown in Figs. 2, 3, 6 and 8. In simulations we used $N_\chi = 4\times10^4$ cells within the range from the TMZ center to the boundary. The initial values of quantities in simulations were ν_0 = 15.7675, E_0 = 0.042, d_0 = 0.0023.

As one can see from Fig. 2, the discrepancy in profiles is insignificant: both 2D simulations nearly coincide, which indicates that they converge with respect to the number of computational cells, and that the flow is sufficiently close to incompressible. The same is valid for the turbulent energy (Fig. 3): an insignificant discrepancy between solution in subsection 2.4 and results of the both 2D simulations (which coincide) is observed.

Eq. (28) should be written in the following form:

$$D = u_0^2 \cdot (t - t_0) \cdot d(\chi), \quad \chi \equiv \frac{y}{u_0 \cdot (t - t_0)}.$$

Here, t_0 is the intersection point of *x* axis and the linear (self-similar) section of dependence $\hat{b}(t) = z_{0.9}(t) - z_{0.1}(t)$ (the line of black dots in Fig. 4a). According to data in Fig. 4a, $t_0 = -0.064$ for N = 400 and N = 1000, and t_0 = 0.285 for N = 200.

Note that there is almost no difference between the results in simulations with N = 400 and N = 1000. The turbulent energy maximum in TMZ as a function of time demonstrates the same behavior: we can see in Fig. 4b that it quickly achieves one and the same constant value in all simulations.

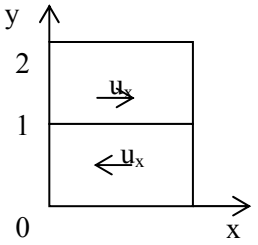

Fig. 1 Initial problem geometry.

Table 5 Options of simulations.

Number of cells along *y* axis	N = 200	N = 400	N = 400	N = 1000
Size of cell	h = 0.01	h = 0.005	h = 0.005	h = 0.002
Pressure (P_0)	10	10	50	10

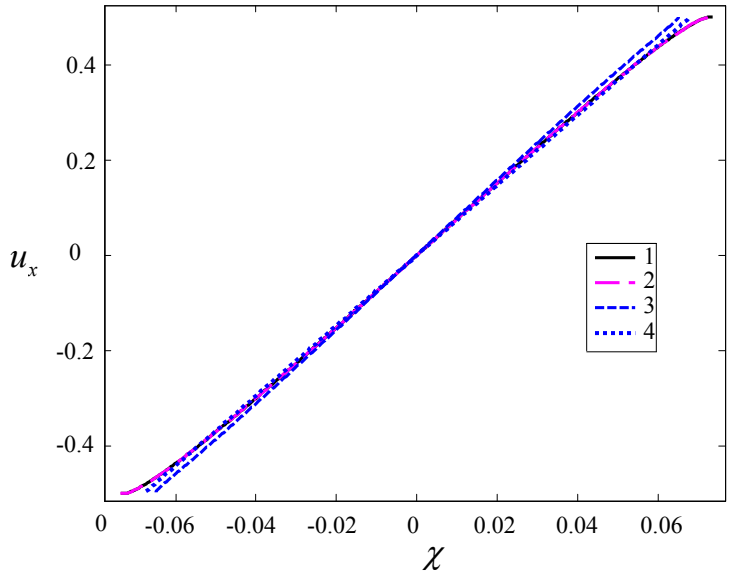

Fig. 2 The velocity profiles in 2D simulations: 1 –N = 1000, P_0 = 10; 2 –N = 400, P_0 = 50; 3 –solution in subsection 3.4; 4 –approximate solution.

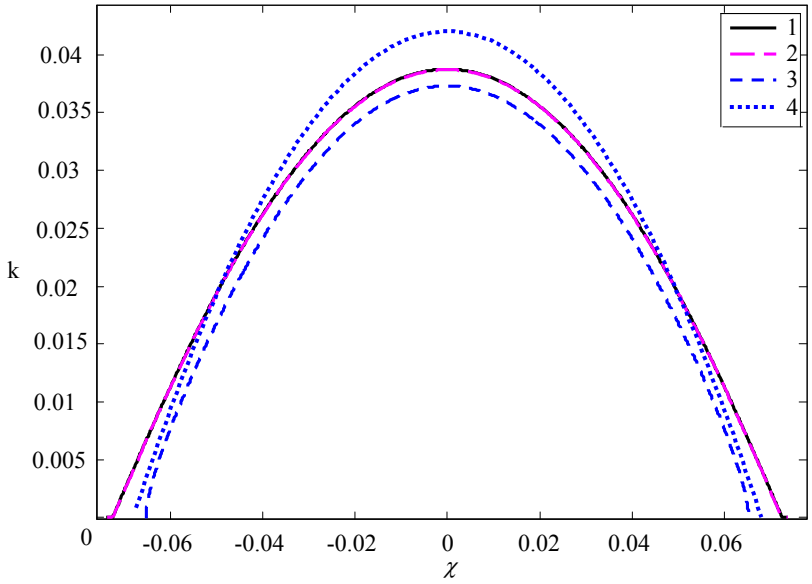

Fig. 3 The turbulent energy profiles. 2D simulations: 1-N = 1000, P_0 = 10; 2-N = 400, P_0 = 50; 3–solution 3.4; 4–approximate solution.

Fig. 5a illustrates function $F_\varepsilon \equiv \varepsilon_m \cdot (t - t_0)$ of the TMZ-maximum value ε_m of the turbulent energy dissipation rate. This function also quickly achieves one and the same constant value. Function $F_D \equiv D_m / (t - t_0)$ of the TMZ-maximum value D_m of the turbulent viscosity coefficient is shown in Fig. 5b. This function also quickly achieves its constant value, which is almost the same in simulations with various N.

It follows from the analysis of this data that we observe convergence of the 2D simulation results obtained by varying the computational grid in use. Simulation results for grid N = 200 insignificantly differ from those for grids N = 400 and N = 1000 (which, in turn, are actually indistinguishable).

We see in Fig. 6 that there is an insignificant discrepancy between the turbulent viscosity coefficient profile calculated with the method in subsection 3.4

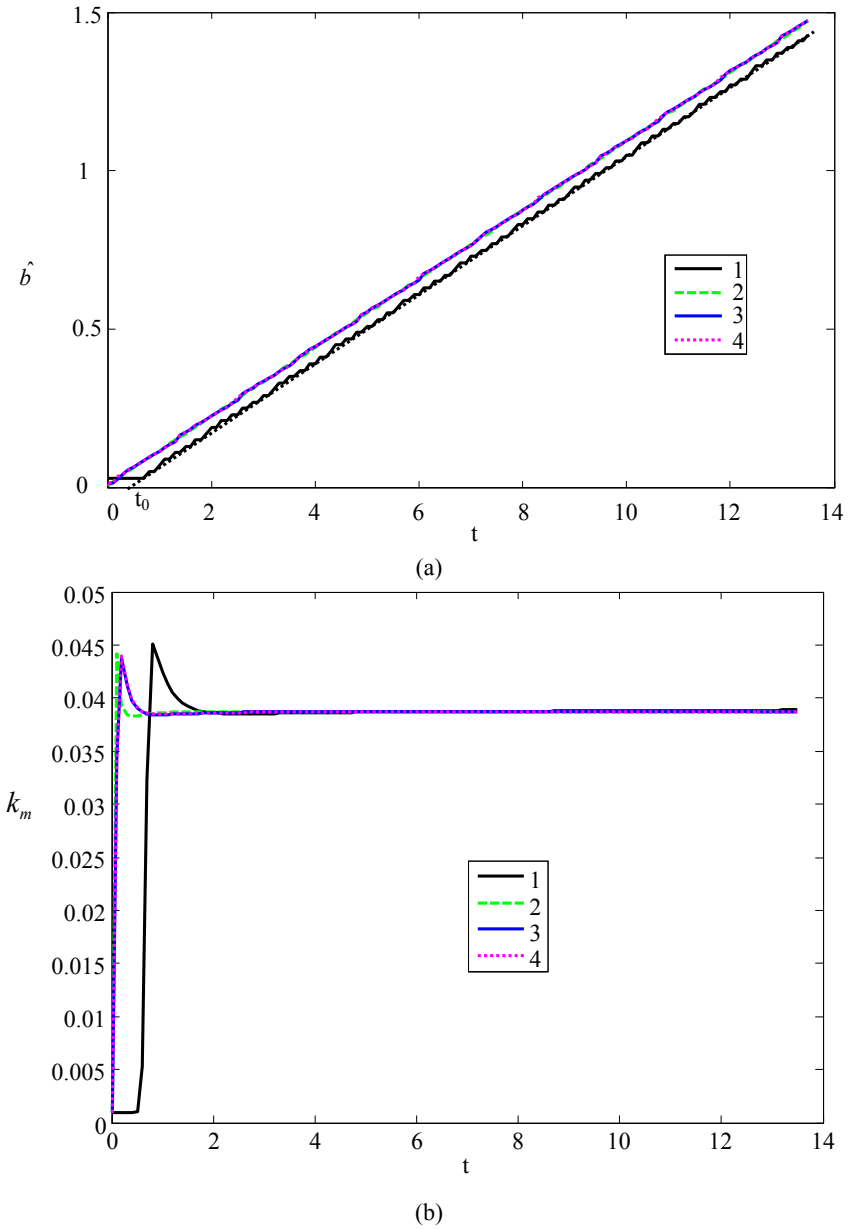

Fig. 4 The turbulent quantities vs time in 2D simulations: (a) TMZ width $\hat{b}$, (b) turbulent energy maximum in TMZ: 1 – P_0 = 10, N = 200; 2 - P_0 = 10, N = 1000; 3 - P_0 = 10, N = 400; 4 – P_0 = 50, N = 400.

and profiles in both 2D simulations (they coincide). There is a satisfactory agreement, in general, with the approximate analytical solution.

In solution 3.4 at the right boundary, both the flux of turbulent energy dissipation rate, $\tilde{\varepsilon} \equiv c_D \cdot e$ and the flux of turbulent energy itself become zeroes (Fig. 7). There is an insignificant discrepancy between the profiles of turbulent energy dissipation rate in solution 3.4 and in 2D simulations (which are almost coincident) (Fig. 8).

The integrated data obtained by solving the system of ordinary differential Eqs. (30)-(33) describing the self-similar regime of shear flow are as follows:
from subsection 3.4:

$$\beta = b/\left(u_0 \cdot t\right) \equiv \Delta\chi_b = 0.1105, k_m = \max(k) = 0.0373. \quad (47)$$

Here, according to the definition in Refs. [9, 10], $b = z_{0.95} - z_{0.1}$ is the TMZ width found for level

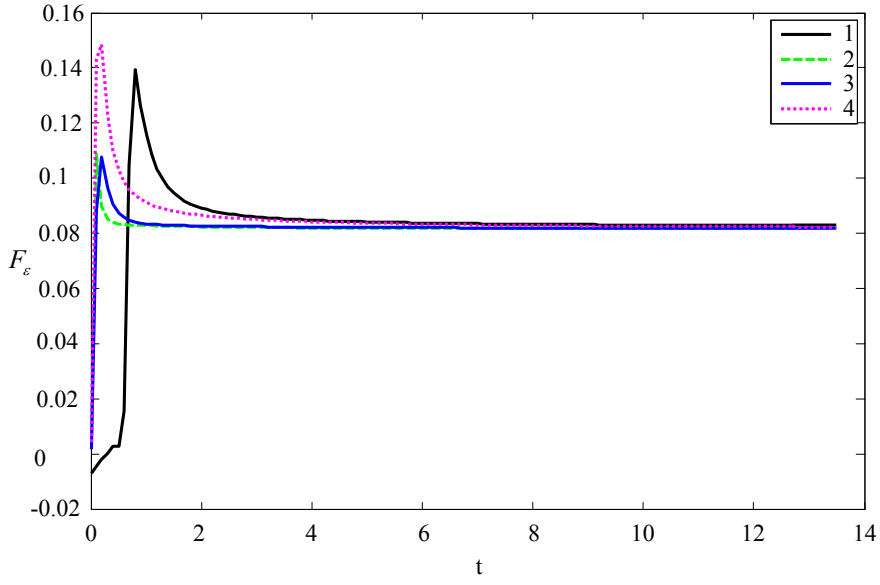

(a)

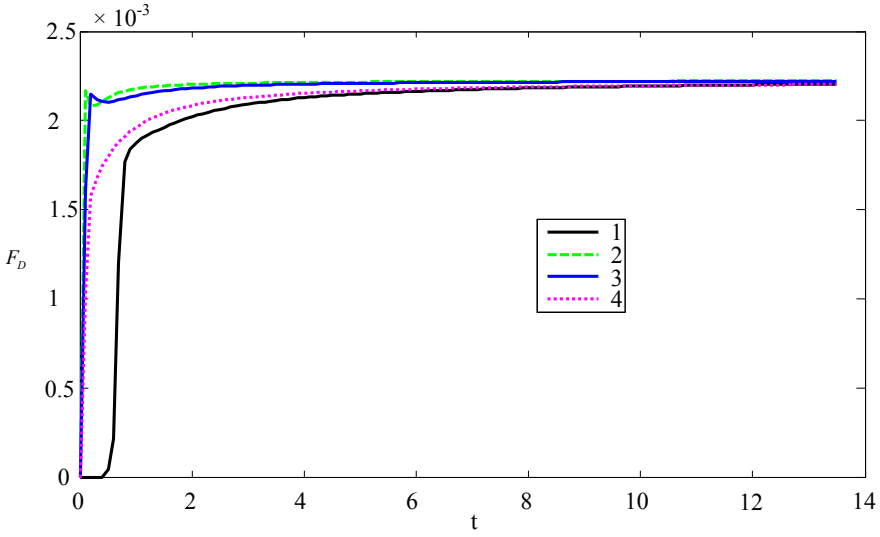

(b)

Fig. 5 TMZ-maximum value of turbulent quantities vs time in 2D simulations: (a) the function of turbulent energy dissipation rate, (b) the turbulent viscosity coefficient function: 1 – P_0 = 10, N = 200; 2 - P_0 = 10, N = 1000; 3 - P_0 = 10, N = 400. 4 –P_0 = 50, N = 400.

$$\frac{u_x}{u_0}(z_{0.95}) = \frac{u_x}{u_0}(\chi_{0.45}) = 0.45$$

and

$$\frac{u_x}{u_0}(z_{0.1}) = \frac{u_x}{u_0}(\chi_{-0.4}) = -0.4,$$

or in the spacer plate's coordinate system:

$$\frac{\tilde{u}_x}{u_0}(z_{0.95}) = 0.95 \quad \text{and} \quad \frac{\tilde{u}_x}{u_0}(z_{0.1}) = 0.1.$$

The values in Eq. (47) are close both to the results of 2D simulations with the k-ε model (β = 0.1154, k_m = 0.0388) and results of the approximate analytical solution (β = 0.1156, k_m = 0.042). The β value in (47) also agrees with the 3D ILES results in [4, 5], 3D LES results in [12] and 3D DNS results in [13, 14] (see Appendix A) and measurement results in [9] (see Appendix B). The maximum values of turbulent energy in all the 2D simulations are close and do not contradict the available measurement results.

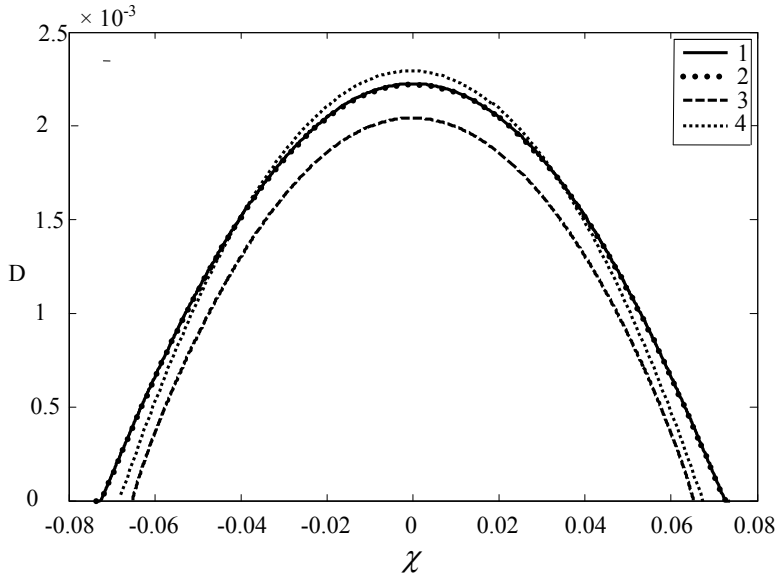

Fig. 6 The turbulent viscosity coefficient profiles in 2D simulations: 1 – N = 1000, P_0 = 10; 2 – N = 400, P_0 = 50; 3 – solution 3.4; 4 – approximate analytical solution.

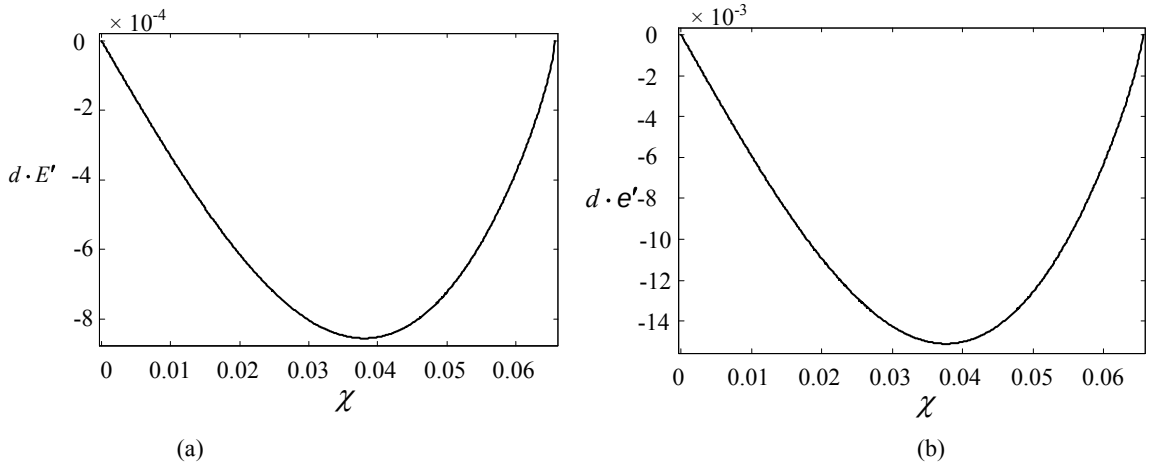

Fig. 7 Profiles of the turbulent energy flux (left) and dissipation rate flux (right) in solution 3.4.

Thus, the velocity profiles in 2D simulations satisfactorily agree with results of the numerical integration of ordinary differential equations (29)-(32) describing the self-similar regime of shear flow and with the approximate analytical solution, as it is clearly seen in Figs. 2, 3, 6 and 8.

4. Discussion of results and conclusions

The 2D EGAK code results of the numerical simulation using the k-ε model demonstrate quick transition to the self-similar regime, the initial values of k and ε are forgotten. This regime is characterized by a linear growth of TMZ width with time and by time-constant maxima of turbulent energy in TMZ (k_m) and functions of its dissipation rate (ε_m), as well as the turbulent viscosity coefficient (D_m): $\varepsilon_m(t - t_0)$ and D_m/t.

A system of ordinary differential equations has been constructed for the self-similar regime of shear flow and the equation system solution methods are presented. The solutions found are in a good agreement with the 2D EGAK code simulation results. Thus, they can be used for the code verification.

The obtained solutions agree with the approximate analytical solution and, hence, it can be used for the preliminary selection of the k-ε model coefficients

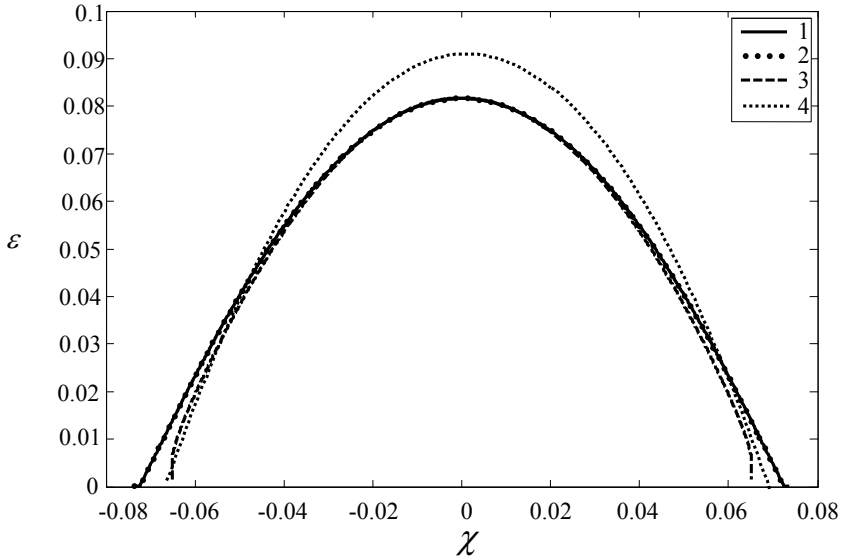

Fig. 8 Profiles of the dissipation rate coefficient of turbulent energy: simulations: 1 – N = 1000, P_0 = 10; 2 – N = 400, P_0 = 50; 3 – solution 3.4, 4 – approximate analytical solution.

$\sigma_k, c_\mu, \sigma_\varepsilon, c_{\varepsilon 1}, c_{\varepsilon 2}$, if there is a need to change one, or several coefficients to specify data of experiments, or 3D simulations for the particular flow.

In the present work, we obtained β = 0.116 in 2D simulations with coefficients from paper [1], while the solution of self-similar equations gives β = 0.11. The linear fitting for experimental data leads to β = 0.104. The averaged 3D ILES results on finer computational grids are also close to the results obtained in the present work. Thus, the k-ε model coefficients taken in [1] provide a satisfactory description of a plane shear layer of mixing and are preferable, in comparison with the standard coefficients, for describing the gravitational mixing in a plane interfacial layer and a plane light (heavy) layer, as well as the decay of homogeneous isotropic turbulence.

References

[1] Guzhova, A. R., Pavlunin, A. S. and Statsenko. V. P. 2005. "Specification of Constants for the $k-\varepsilon$ Model of Turbulence Based on Results of the Direct Numerical Simulation for the Simplest Turbulent Flows and Measurements." *VANT. ser. TAP* 3: 37-48.

[2] Andronov, V. A., Zhidov, I. G., Meshkov, E. E., Nevmerzhitskii, N. V., Nikiforov, V. V. and Razin, A. N. et al. 1995. "Computational and Experimental Studies of Hydrodynamic Instabilities and Turbulent Mixing." (Review of VNIIEF efforts). LA-12896. CIC-14 Report Collection, Los Alamos National laboratory.

[3] Bakhrakh, S. M., Zhmailo, V. A., Statsenko, V. P. and Yanilkin. Yu. V. 1983. "Numerical Simulation of Turbulent Mixing in Shear Flows." *Numerical Methods of Continuum Mechanics* 14: N2.

[4] Zhmailo, V. A., Stadnik, A. L., Statsenko, V. P. and Yanilkin, Yu.V. 1995. "Direct Numerical Simulation of Turbulent Mixing in Shear Flows." 5th International Workshop on the Physics of Compressible Turbulent Mixing, Stony Brook (USA),

[5] Zhmailo, V. A., Sin'kova, O. G., Statsenko, V. P. and Yanilkin, Yu. V. 2004. "3D Direct Numerical Simulation of Shear Turbulent Mixing." *VANT, ser. TAP* 3: 23-39.

[6] Spenser, B. W. and Jones, B. G. 1971. "Statistical Investigation of Pressure and Velocity Fields in the Turbulent Two-Stream Mixing Layers." -AIAA Paper. 613.

[7] Rodi, W. A. 1975. "Review of Experimental Data of Uniform Density Free Turbulent Boundary Layers. -Studies in Convection." Acad. Press, London.

[8] Browand, F. K. and Latigo, B. O. 1979. "Growth of the Two-Dimensional Mixing Layer." *Phys. Fluids* 22: 1011.

[9] Oster, D. and Wygnanski, I. 1982. "The Forced Mixing Layer between Parallel Streams." *Journal of Fluid Mechanics* 123: 91-130.

[10] Hussain, A. K. M. F. and Zedan, M. F. 1978. "Effects of the Initial Condition on the Axisymmetric Free Shear Layer: Effect of the Initial Fluctuation Level ." *Phys. Fluids* 21 (9): 1100-12

[11] Weisbrot, I., Einav, S. and Wygnanski, I. 1982. "The

Non-Unique Rate of Spread of the Two-Dimensional Mixing Layer." *Phys. Fluids* 25 (10): 1691-3.

[12] Balaras, E., Piomelli, U. and Wallace, J. M. 2001. "Self-Similar States in Turbulent Mixing Layers." *J. Fluid Mech.* 446: 1-24,

[13] Rogers, M. M. and Moser, R. D. 1994. "Direct Simulation of a Self-Similar Turbulent Mixing Layer." *Phys. Fluids* 6: 903-23,

[14] Attili, A. and Bisetti, F. 2012. "Statistics and Scaling of Turbulence in a Spatially Developing Mixing Layer at Reλ = 250." *Physics of Fluids* 24:035109.

[15] Statsenko, V. P., Velitchko, O. M., Yanilkin, Yu. V. and Zharova, G. V. 1999. "Buoyant Jet Formation." 7th International Workshop on the Physics of Compressible Turbulent Mixing, St.-Petersburg, Russia.

[16] Launder, B. E. and Spalding, D.B. 1974. "The Numerical Computation of Turbulent Flows". *Comp. Meth. In Appl. Mech. And Eng.* 3: 269-89.

[17] Rodi, W. 1979. "Influence Buoyancy and Rotation on Equations for the Turbulent Length Scale". Proc. 2nd Symp. on Turbulent Shear Flows.

[18] El Tahry, S. H. 1983. "k-ε Equation for Compressible Reciprocating Engine Flows." *AIAA, J. Energy* 7 (4): 345-53.

[19] Llor, A. 2005. "Statistical Hydrodynamic Models for Developed Mixing Instability Flows." *Lect. Notes Phys.* Springer, Berlin Heidelberg.

[20] Landau L.D., Lifshitz E.M. Continuum Mechanics. - M.: GITTL, 1953.

[21] Paavo. S. 1976. "Two-Point Turbulent Measurements Downstream of a Heated Grid." *Phys. Fluids* 19: 1876.

[22] Tennekes H. 1973. "Similarity Laws and Scale Relations in Planetary Boundary Layers." AMS Workshop on micrometeorology. Science Press, Boston.

[23] Read, K. I. 1984. "Experimental Investigation for Turbulent Mixing by Rayleigh-Taylor Instability." Physica D12, 45.

[24] Kucherenko, Yu. A., Shibarshov, L. I., Chitaikin, V. I., Balabin, S. I. and Pylaev, A. P. 1991. "Experimental Study of Asymptotic Stage of the Gravitational Turbulent Mixing Self-Similar Mode." In *Proceedings of the 3rd International Workshop on Physics Compressible Turbulent Mixing*.

[25] Linden, P. F., Redondo, J. M. and Youngs, D. L. 1994. "Molecular Mixing in Rayleigh-Taylor Instability." *J. Fluid Mech.* 265: 97-124.

[26] Kucherenko, Yu. A., Shestachenko, O. E., Piskunov, Yu. A., Sviridov, E. V., Medvedev, V. M. and Baishev, A. I. 2001. "Experimental Investigations of the Self-Similar Regime of Different-Density Gas Mixing in the Earth Gravity Field." Presentation at VI Zababakhin Scientific Readings, Snezhinsk, Russia.

[27] Dimonte, G. and Schneider, M. 2000. "Density Ratio Dependence of Rayleigh-Taylor Mixing for Sustained and Impulsive Acceleration Histories." *Physics of Fluids* 12 (2): 304-21.

[28] Anisimov, V. I., Kozlovskikh, A. S. and Baban, S. A. 2003. "Analysis of Results for Experiments on Turbulent Mixing with Moderate Reynolds Numbers in the Earth Gravity Field." Presentation at VI Zababakhin Scientific Readings, Snezhinsk, Russia.

[29] Olson, D. H. and Jacobs, J. W. 2009. "Experimental Study of Rayleigh-Taylor Instability with a Complex Initial Perturbation." *The Physics of Fluids* 21: 034103.

[30] Youngs, D. L. 1994. "Numerical Simulation of Mixing by Rayleigh-Taylor and Richtmyer-Meshkov Instabilites." *Laser and Particle Beams* 12 (4): 725-50.

[31] Zhmailo, V. A., Stadnik, A. L., Statsenko, V. P. and Yanilkin, Yu. V. 1996. "Direct Numerical Simulation of Gravitational Turbulent Mixing." *VANT. Ser. TAP.* 1-2: 29-37.

[32] Sin'kova, O. G., Stadnik, A. L., Statsenko, V. P., Yanilkin, Yu. V. and Zhmailo, V. A. 1997. "Three-Dimensional Direct Numerical Simulation of Gravitational Turbulent Mixing." In *Proceeding of 6th International Workshop on the Physics of Compressible Turbulent Mixin*g. Marseille, France.

[33] Yanilkin, Yu. V., Statsenko, V. P., Rebrov, S.V., Sin'kova, O. G. and Stadnik, A. L. 2001. "Study of Gravitational Turbulent Mixing at Large Density Differences Using Direct 3D Numerical Simulation." Report to 8th International Workshop on the Physics of Compressible Turbulent Mixing : 8th IWPCTM, Pasadena, CA, USA.

[34] Dimonte, G., Dimits, A., Weber, S. and Youngsy, D. L. et. al. 2001. "A Comparison of High-Resolution 3D Simulations of Turbulent Rayleigh-Taylor Instability: Alpha-Group Collaboration." Report to 8th International Workshop on the Physics of Compressible Turbulent Mixing: 8th IWPCTM, Pasadena, CA, USA.

[35] Weber, S. V., Dimonte, G. and Marinak, M. M. 2001. "ALE Simulation of Turbulent Rayleigh-Taylor Instability in 2-D and 3-D: Alpha-Group Collaboration." Report to 8th International Workshop on the Physics of Compressible Turbulent Mixing: 8th IWPCTM, Pasadena CA, USA.

[36] Kucherenko, Yu. A., Balabin, S. I. and Pylaev, A. P. 1993. "Experimental Study of Asymptotic Stage of the Gravitational Turbulent Mixing of Thin Liquid Layers of Different Densities." Report to 4th International Workshop on the Physics of Compressible Turbulent Mixing. Cambridge, England.

Appendix A: Review of experimental data on shear mixing.

Consider homogeneous flows coming from a spacer plate at velocities u_1 and u_2. It is precisely these tests that have been used to study a plane mixing layer and described, in particular, in papers [9-11]. It is assumed that density is uniform in the problem. Thus, the problem is one-dimensional in coordinates of fluid, but it is time-dependent, because in the self-similar regime the plane mixing layer's width grows linearly with time in proportion to the difference u_0 between the jet velocity and the surrounding medium velocity

$$b = \beta \cdot u_0 \cdot t .$$

Here, according to the definition in [9-11], $b = y_{0.95} - y_{0.1}$ is the TMZ width determined for level $\frac{u_x}{u_0}(z_{0.95}) = \frac{u_x}{u_0}(\chi_{0.45}) = 0.45$ and $\frac{u_x}{u_0}(z_{0.1}) = \frac{u_x}{u_0}(\chi_{-0.4}) = -0.4$, or in the spacer plate coordinates: $\frac{\tilde{u}_x}{u_0}(z_{0.95}) = 0.95$ and $\frac{\tilde{u}_x}{u_0}(z_{0.1}) = 0.1$. Quantity β should be represented using quantity $b' \equiv db/dx = b/(x - x_0)$, which is measured directly in experiments.

With regard to $x - x_0 = (u_1 + u_2)/2 \cdot t$ and $u_0 = u_2 - u_1$, we obtain

$$\beta = \frac{b'}{2\lambda}, \text{ where } \lambda \equiv \frac{u_2 - u_1}{u_2 + u_1},$$

as defined in [9]-[11]. In other words, with regard to $m \equiv u_1 / u_2$ the expression for β can be written as

$$\beta = \frac{b'}{2} \cdot \frac{(1+m)}{(1-m)}.$$

Paper [9] gives the b' values calculated by various authors for different values of λ. We present this data (see Table A_1) for $\lambda \lesssim 0.54$ (these values are not too large) corresponding to $m \gtrsim 0.3$.

Table A_1 Experimental data from [9] for the mixing rate.

λ	m	β
0.1474	0.743	0.120
0.2470	0.604	0.071
0.2515	0.598	0.105
0.2546	0.594	0.084
0.2553	0.593	0.095
0.2561	0.592	0.087
0.3366	0.496	0.094
0.4316	0.397	0.085
0.4324	0.396	0.094
0.4324	0.396	0.093
0.4430	0.386	0.112
0.5380	0.300	0.084
0.5418	0.297	0.094

Fig. A1 illustrates experimental data in the form of plots for *β(m)* function**.** Measurement results are approximated with the linear dependence

$$\beta = 0.0196 \cdot m + 0.084 \qquad \text{(A1)}$$

With m=1 we obtain β=0.1036 (see also Fig. A1). The root-mean-square deviation of experimental data from straight line (A1) is $\delta\beta = \left\langle \left(\langle \beta \rangle - \beta \right)^2 \right\rangle^{1/2}$ ≈0.023 (here, symbols $\langle\ \rangle$ mean "averaging"), it is shown in Fig. A1. As one can see, with $m \to 1$ there

is a satisfactory agreement with the 2D simulation results. Remember that our temporal mixing layer studies described in this paper correspond to experimental investigations for the spatially evolving configuration in the limit of m →1.

Paper [9] also presents results of various authors, who measured maximum values of root-mean-square fluctuations of different velocity components (see Table A_2). The turbulent energy values calculated using these measurement results are also given in this table.

These results agree with all the simulation results presented in the present paper.

Results of 2D simulations and self-similar solutions 3.4 are also illustrated by Fig. A2, which shows the reciprocal of growth rate of the mixing layer's width:

$$\sigma = \frac{1.855\Delta x}{\Delta\left(z_{0.1} - z_{0.9}\right)},$$

where, $\Delta\left(z_{0.1} - z_{0.9}\right)$ is the distance between two points, at which relative velocity $\hat{u} = \left(u - u_2\right) / \left(u_1 - u_2\right)$ equals 0.1 and 0.9.

Similar to [3], the jet length ($x-x_o$) in experiments is assumed to be correspondent to time ($t - t_0$): $(x - x_o) = (u_1 + u_2) / 2 \cdot (t - t_o)$. Since $\Delta z = u_0 \cdot (\chi_{0.4} - \chi_{-0.4}) \cdot (t - t_o) = 2u_0 \cdot \chi_{0.4} \cdot (t - t_o)$, we have

$$\sigma = \frac{1.855 \cdot (1+m)}{4 \cdot (1-m) \cdot \chi_{0.4}} = \frac{1.855}{4 \cdot \lambda \cdot \chi_{0.4}},$$

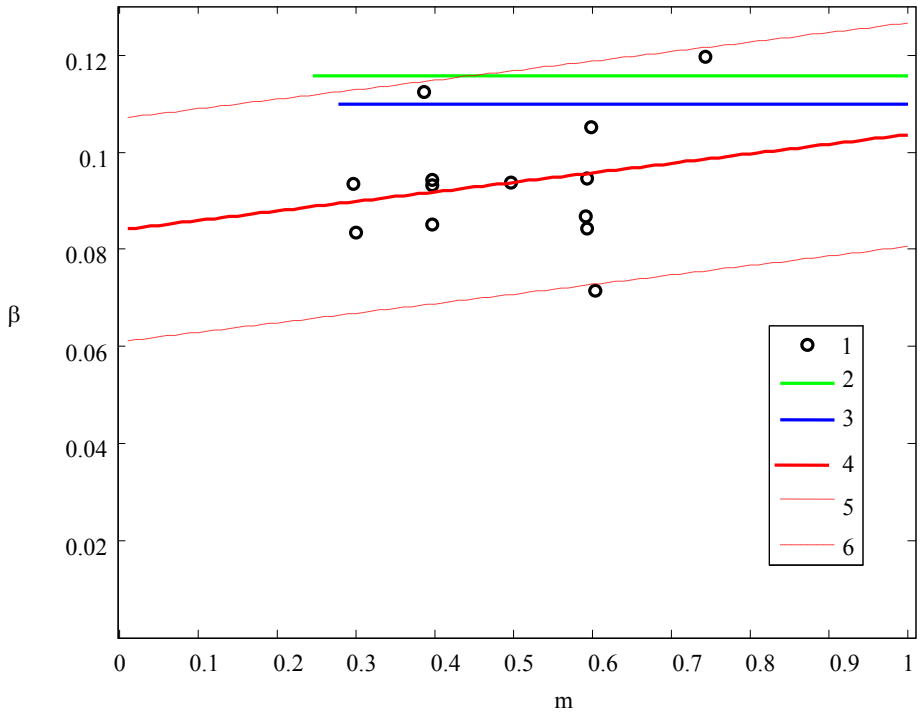

Fig. A1 The mixing rate in a plane layer vs velocity ratio. 1 – experimental data of various authors from paper [9] and linear fitting (4), 5-6 – approximation with root-mean-square deviation; 2 – 2D simulations; 3 – solution of self-similar equations.

Table A_2 The root-mean-square fluctuations of velocity components.

Authors	u'_x / u_0	u'_y / u_0	u'_z / u_0	k_m
Spencer 1970	0.17	0.14	0.145	0.0348
Yule 1971	0.173	0.16	0.18	0.044
Oster, Wygnanski 1982	0.18	0.153	0.145	0.0384

where, $m \equiv u_1 / u_2$ and velocities are associated with the coordinate system of a spacer plate, or a nozzle. Similarly, Fig. A2 illustrates data of measurements from [8] within the range of *m* values corresponding to the range of λ values. Points in Fig. A2 show experimental data of various authors from paper [7].

One can see that the calculated curves agree with measurement results. The best agreement is observed at large *m* values, which correspond to the considered problem to a higher extent.

Appendix B: Review of the direct 3D numerical simulation results for shear mixing.

Papers [4, 5] give the 3D ILES results for different values of N_x (the number of cells in the flow motion direction). We present this data in Table A_3 after additional post-processing efforts. The TMZ width in the papers above, $\Delta\left(z_{0.1} - z_{0.9}\right)$ is the distance between two points, at which relative velocity $\hat{u} = \left(u - u_2\right) / \left(u_1 - u_2\right)$ equals 0.1 and 0.9. However, according to the definitions in [9, 11], we take $b = z_{0.95} - z_{0.1}$, i. e. the TMZ width for level $\frac{u_x}{u_0}(z_{0.95}) = \frac{u_x}{u_0}(\chi_{0.45}) = 0.45$ and $\frac{u_x}{u_0}(z_{0.1}) = \frac{u_x}{u_0}(\chi_{-0.4}) = -0.4$, or in the spacer plate coordinates: $\frac{\tilde{u}_x}{u_0}(z_{0.95}) = 0.95$ and $\frac{\tilde{u}_x}{u_0}(z_{0.1}) = 0.1$. In this case, we obtain the values of $\beta = \frac{b}{u_0 \cdot \left(t - t_0\right)}$ given in Table A_3.

Besides, the post-processing of the 3D ILES results from [12] and DNS results from [13] gives us β=0.064÷0.08 and β=0.077, respectively. Similar to our simulations, their simulations were performed for a temporal mixing layer. Simulations with the 3D DNS method in [14] were performed for a spatially evolving configuration. Regarding that *m* in [14] equals u_1/u_2=1/3, we have $\beta = 0.5b'\left(1+m\right) / \left(1-m\right) = b'$. Here, $b' \equiv db/dx = \Delta y / \Delta x = r_\theta \cdot \Delta y^+$, $r_\theta = \Delta\theta / \Delta x = 0.0168$ according to [14]. $\Delta y^+ = \Delta y / \Delta\theta$ is found using the velocity profiles from [14] and, as a result, we obtain $\beta = 0.086 \div 0.093$ for data in [14]. These results agree with the data in [4-5].

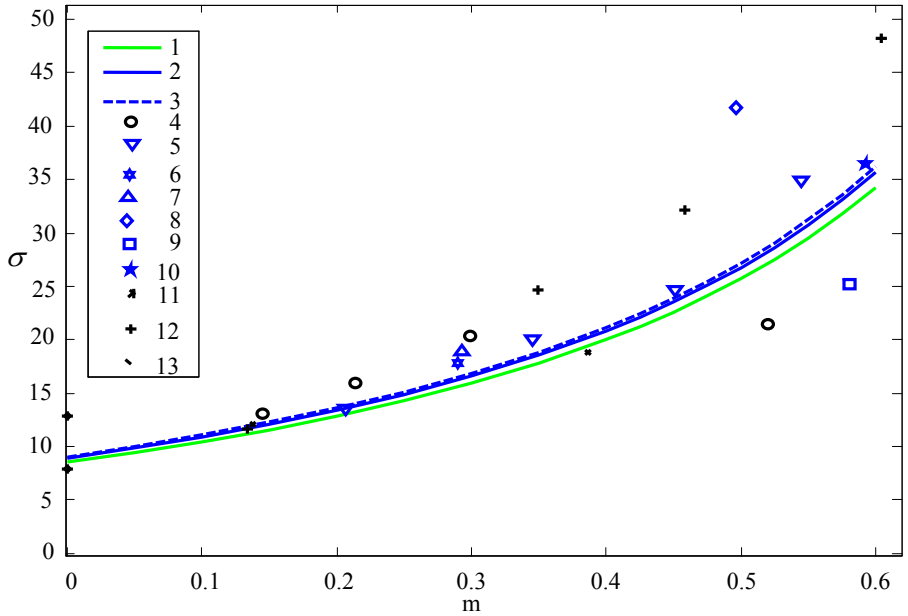

Fig. A2 Quantity σ as a function of time in the problem of a shear mixing layer. Present paper: 1 – 2D simulations; 2 – solution 2.4. 3÷4 –measurements [8], 5÷12 – experimental data of various authors from Ref. [7].

Table A_3 The integral 3D ILES values.

Option No.	Number of cells	L_z	L_x	β	k_m
1	100^3	1	1	0.077 ÷ 0.09	0.033-0.037
2	100^3	1	1	0.07 ÷ 0.1	0.027
3	100^3	1	1	0.096	0.036
4	$150^2 \times 200$	2	1.5	0.1 ÷ 0.1075	0.038 ÷ 0.041
5	$200^2 \times 400$	2	1	0.098 ÷ 0.1	0.038 ÷ 0.04
6	$300^2 \times 400$	2	1.5	0.086 ÷ 0.1	0.033 ÷ 0.035
7	$300^2 \times 400$	2	1.5	0.13-0.17	0.05

Fig. A3a illustrates the data from [4-5] as a plot of function $\beta(N_x)$. The linear fitting of this data is

$$\beta = 1.665 \cdot 10^{-4} \cdot N_x + 0.07115 . \tag{A2}$$

With N_x=300 we have β=0.121 (see also Fig. A3). The root-mean-square deviation from straight line (A2) is $\delta\beta = \left\langle \left(\langle \beta \rangle - \beta \right)^2 \right\rangle^{1/2}$ ≈0.024, it is shown in Fig. A3. One can see a satisfactory agreement with the 2D simulation results and solutions of self-similar equations.

Fig. A3b illustrates 3D simulation results for the maximum turbulent energy in the form of $k_m(N_x)$ function plots. The linear fitting of this data is

$$k_m = 2.873 \cdot 10^{-5} \cdot N_x + 0.03178 . \tag{A3}$$

In this case, the root-mean-square deviation of results from straight line (A3) is $\delta k_m = \left\langle \left(\langle k_m \rangle - k_m \right)^2 \right\rangle^{1/2}$ ≈0.0055, it is shown in Fig. A3b. As one can see, there is a satisfactory agreement with all results of 2D simulations and self-similar equation solutions.

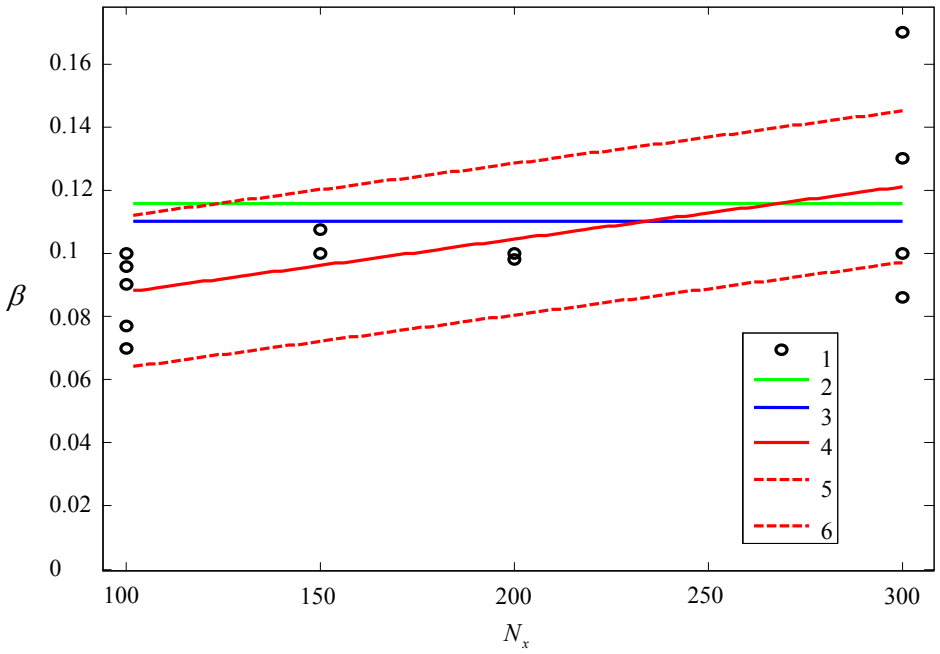

(a)

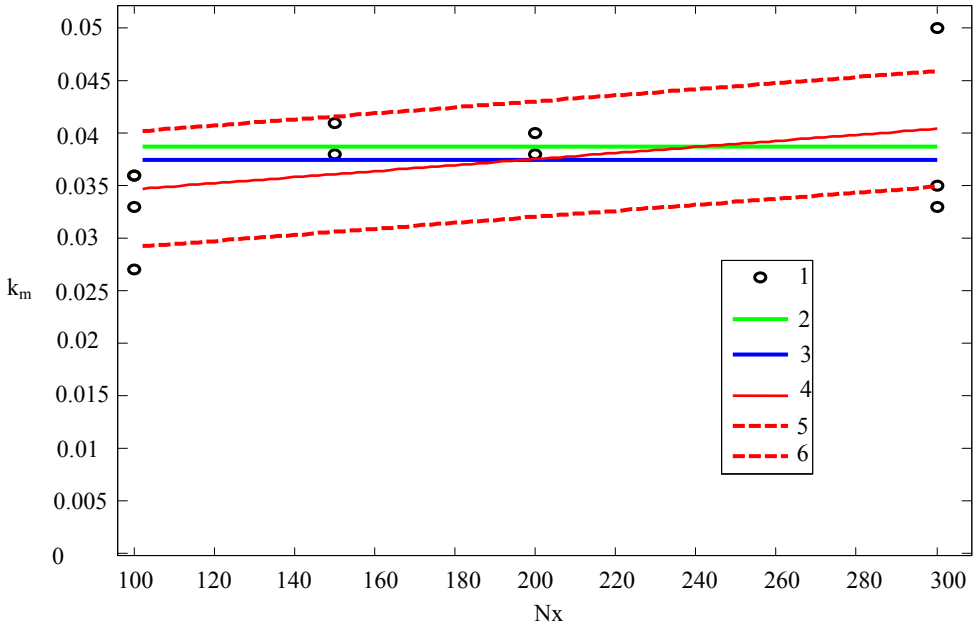

(b)

Fig. A3 The mixing rate of a plane layer (a) and the maximum turbulent energy in TMZ (b) vs. the number of computational cells. 1 – 3D ILES results and linear fitting (4); 5-6 –fitting with RMS deviation; 2 – 2D simulations; 3 – solution of self-similar equations.